

The Structure of Titan's Wake From Plasma Wave Observations

D. A. GURNETT¹, F. L. SCARF², AND W. S. KURTH¹

During the Voyager 1 flyby of Saturn's moon Titan, the plasma wave instrument detected several types of plasma wave emissions. On the inbound leg a broad region of intense low-frequency noise was detected on the side of Titan facing away from Saturn. This noise has characteristics similar to the electric field turbulence observed in the magnetosheath at the earth and the ionosheath at Venus and is believed to be generated by newly created ions that are being accelerated in the vicinity of Titan by the corotational electric field. During the pass through the induced magnetic tail of Titan, a series of upper hybrid resonance emissions were observed. The electron density profile inferred from these emissions shows three distinct peaks with densities of $\sim 40 \text{ cm}^{-3}$, the first peak corresponding to the entry into the magnetic tail, the second peak corresponding to the neutral sheet crossing from the northern to the southern tail lobe, and the third, somewhat smaller, peak corresponding to the outbound exit from the tail. Large depressions in the magnetic field strength are observed coincident with each of the density peaks. These effects indicate that a dense plume of plasma is being carried downstream of Titan by the interaction with the rapidly rotating magnetosphere of Saturn. By equating the magnetic field pressure in the tail lobe to the plasma pressure in the neutral sheet, the temperature of the plasma is estimated to be about 8600°K. This low temperature suggests that the plasma originates from the ionosphere of Titan, probably forming a plume of plasma with a θ or H cross section extending downstream from Titan. Within the tail lobes, a second type of low-frequency electric field noise was observed, with characteristics very similar to a type of noise called broadband electrostatic noise, which is found in the earth's magnetic tail. As in the case of the earth, this noise is most intense near the outer boundary of the plasma sheet and is almost completely absent in the high-density region near the neutral sheet.

1. INTRODUCTION

One of the principal objectives of the Voyager 1 encounter with Saturn on November 12-13, 1980, was a close flyby of the moon Titan. This moon was considered an important target for investigation because it is the only moon in the solar system known to have a substantial atmosphere. Because Titan's orbit at $20.2 R_S$ is near the nominal stand-off distance for the Saturnian magnetopause [Smith *et al.*, 1980; Acuna and Ness, 1980], Titan can interact with either the magnetosphere or the solar wind, depending on its orbital position and the instantaneous magnetopause position. Because it was not known ahead of time whether Titan would be in the solar wind or magnetosphere at the time of the flyby, a trajectory was chosen that passed through the nominal positions for both the solar wind wake and the magnetospheric wake. At the time of the Voyager 1 flyby, Titan was located inside of the magnetosphere at a local time of about 1330, and an extended magnetospheric wake region was observed downstream of Titan.

Figure 1 shows the spacecraft trajectory in a Titan-centered coordinate system and the direction of the nominal corotational plasma flow induced by Saturn's rotation, assuming rigid rotation. At closest approach the radial distance to the center of Titan was $2.53 R_T$, where we use $R_T = 2570 \text{ km}$ [Tyler *et al.*, 1981] for the radius of Titan. As can be seen, Voyager 1 passed almost directly through the geometric center of the wake. All of the particles and fields experiments registered pronounced effects as the spacecraft passed through the magnetospheric wake region [Ness *et al.*, 1981; Bridge *et al.*, 1981; Gurnett *et al.*, 1981; Krimigis *et al.*, 1981; Vogt *et al.*, 1981], indicating that a very complex and interesting interaction is occurring between Titan and the magnetosphere of Saturn.

In this paper we present a detailed analysis of the plasma wave emissions detected by the Voyager 1 plasma wave instrument in the vicinity of Titan. This study is intended to supplement and extend the initial report of the Titan plasma wave observations given by Gurnett *et al.* [1981]. For a description of the Voyager plasma wave experiment, see the instrumentation description given by Scarf and Gurnett [1977]. As discussed by Gurnett *et al.* [1981], three principal types of plasma wave emissions were detected in the vicinity of Titan: (1) a band of electrostatic emissions near the local upper hybrid resonance frequency; (2) a broad band of low-frequency electric field noise in a region tentatively identified as a 'sheath' on the inbound and outbound passes through the wake; and (3) high-frequency radio emissions. These three types of emissions are shown in the 16-channel electric field intensity plot of Figure 2, which has been taken from the initial report of Gurnett *et al.* [1981] to provide an overview of the plasma wave observations near Titan. The upper hybrid resonance emissions were used to obtain the electron number density profile indicated by the dashed line. In this paper the main emphasis will be on a critical analysis of the electron density profile obtained from the upper hybrid emissions and on the interpretation of the low-frequency electric field noise.

2. UPPER-HYBRID RESONANCE EMISSIONS

During the pass through the wake, a series of narrow-band electric field emissions was detected in the upper five frequency channels of the spectrum analyzer. These emissions are circled in Figure 2 and identified as 'UHR emissions.' The identification of these emissions with the local upper-hybrid resonance (UHR) frequency is based on the close similarity to upper hybrid resonance emissions observed in the terrestrial and Jovian magnetospheres. The upper hybrid resonance is an electrostatic resonance which occurs at a frequency $f_{\text{UHR}} = (f_p^2 + f_g^2)^{1/2}$, where f_p and f_g are the electron plasma frequency and gyrofrequency. The resonance occurs for electric fields polarized perpendicular to the static magnetic field. In the terrestrial magnetosphere,

¹ Department of Physics and Astronomy, The University of Iowa, Iowa City, Iowa 52242

² TRW Defense and Space Systems, Redondo Beach, California 90278

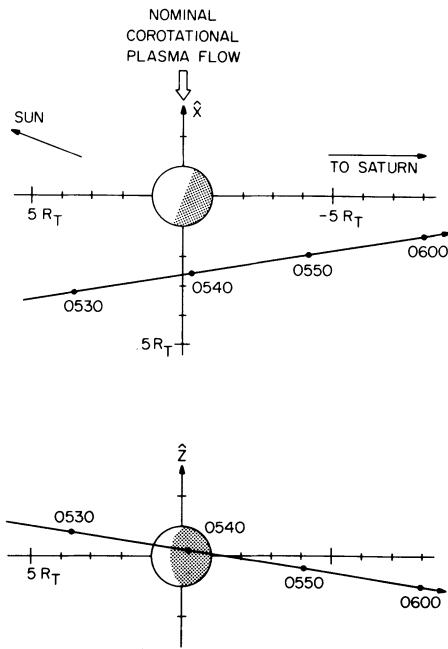


Fig. 1. The Voyager 1 trajectory in Titan-centered coordinates. The Z axis is parallel to Saturn's rotational axis and the X axis is parallel to the nominal corotational plasma flow, assuming rigid rotation. The radius of Titan R_T is taken to be 2570 km [Tyler et al., 1981].

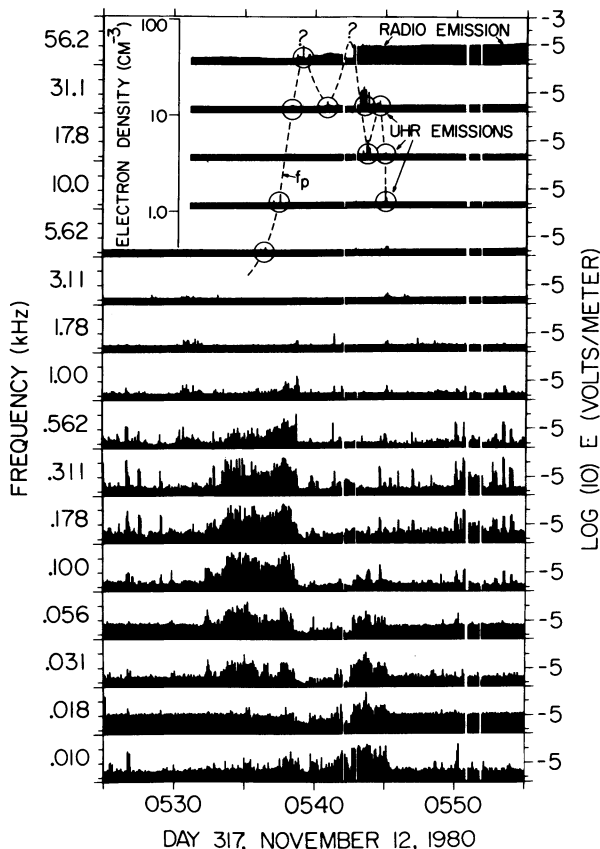


Fig. 2. A survey of all of the plasma wave electric field intensities in the vicinity of Titan. The bandwidths are $\pm 15\%$ for the lowest eight frequencies and $\pm 7.5\%$ for the highest eight frequencies, and the time resolution for the individual intensity measurements is 4 s. Several types of plasma wave effects were detected, including upper hybrid resonance (UHR) emissions, two types of low-frequency electric field noise at frequencies below 1 kHz, and radio emissions from Saturn at 56.2 kHz.

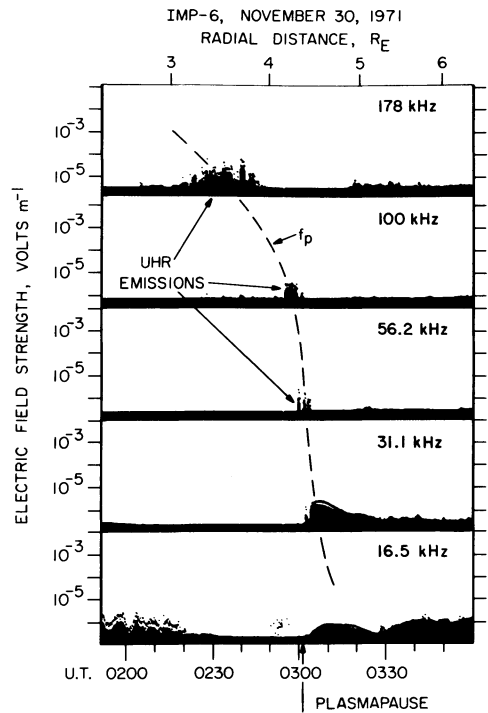


Fig. 3. An example of upper hybrid resonance (UHR) emissions observed near the terrestrial plasmopause by IMP 6. The emission frequency occurs very close to the electron plasma frequency f_p shown by the dashed line. These emissions are believed to be essentially identical to the UHR bands observed near Titan and provide the basis for identifying the narrow-band Titan emissions as upper hybrid resonance emissions.

electrostatic emissions associated with the local upper hybrid resonance have been observed for many years by rocket- and satellite-borne plasma wave instruments [Walsh et al., 1964; Hartz, 1970; Mosier et al., 1973; Shaw and Gurnett, 1975; Hubbard and Birmingham, 1978; Rönmark et al., 1978; Christiansen et al., 1978; Kurth et al., 1979]. Although the detailed characteristics vary somewhat in different regions of the magnetosphere, the common feature is that a narrow-band electrostatic emission occurs near the local upper hybrid resonance frequency. Since the upper hybrid resonance frequency depends on the electron plasma frequency $f_p = 9\sqrt{n_e}$ kHz, where n_e is the electron number density in cm^{-3} , a measurement of the emission frequency together with knowledge of the electron gyrofrequency (from the magnetic field strength) provides a determination of the electron density. For the special case when $f_p \gg f_g$, which is valid for the Titan flyby, the upper-hybrid resonance is essentially coincident with the electron plasma frequency, so that $f_{\text{UHR}} \approx f_p = 9\sqrt{n_e}$ kHz.

To illustrate the close similarity between the Titan emissions and the terrestrial UHR emissions, Figure 3 shows an example of UHR emissions observed by the IMP 6 spacecraft during an outbound pass through the terrestrial plasmopause [from Shaw and Gurnett, 1975]. This example has been selected because the filter bandwidth and instrumental characteristics are nearly identical to the Voyager instrumentation. The UHR emissions in this case occur as a single narrow-band emission line which sweeps downward in frequency as the spacecraft crosses the plasmopause. The approximate variation of the electron plasma frequency and upper-hybrid resonance frequency $f_p \approx f_{\text{UHR}}$ is shown by the

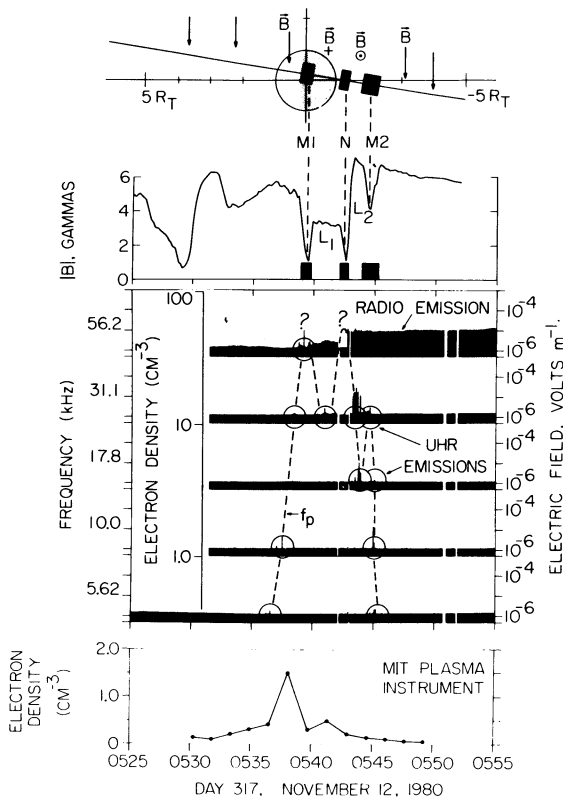


Fig. 4. The bottom panel shows the electron density (dashed line) inferred from the upper hybrid resonance frequency, and the top panel summarizes the magnetic field directions (arrows) and intensities from the magnetic field instrument [Ness *et al.*, 1981]. Three distinct peaks occur in the electron density profile, the first at the entry (M1) into the magnetic tail of Titan, the second at the neutral sheet crossing (N), and the third at the exit (M2) from the tail.

dashed line. Magnetic field measurements confirm that this emission has no magnetic field component and is therefore electrostatic, at least to within the limits imposed by the instrument sensitivity. Other measurements [Kurth *et al.*, 1979] have shown that the electric field is polarized perpendicular to the magnetic field, thereby confirming that the electric field has the correct polarization for the UHR interpretation. The polarization measurements are important because they eliminate an alternative interpretation that the emissions are electron plasma oscillations at the local electron plasma frequency.

As can be seen from a comparison of Figures 2 and 3, the narrow-band emissions observed at Titan bear a strikingly close resemblance to the UHR emissions observed in the terrestrial magnetosphere. In both cases the emissions occur in a narrow frequency band, the center frequency of which varies systematically with spatial position. The maximum electric field amplitudes, $\sim 10^{-6}$ to 10^{-4} V m⁻¹, are quite comparable, and the intensity variations have a similar 'spiky' structure on a time scale of a few seconds. These close similarities are the basis for identifying the narrow-band Titan emissions with the upper-hybrid resonance. Because the UHR emissions provide a crucial measurement of the electron density profile through Titan's wake, it is important to comment on the degree of certainty to which we can identify this emission as the upper hybrid resonance. Unfortunately, it is not possible to identify the plasma wave mode with the high degree of certainty available in the

terrestrial observations because the Voyager plasma wave instrument does not provide polarization or magnetic field measurements. Nevertheless, we feel very confident that the mode identification is essentially correct and that the electron density can be computed by using $f_{UHR} \approx f_p = 9\sqrt{n_e}$ kHz. The strongest argument supporting this interpretation is based on a simple listing of the possible wave modes in the frequency range of interest. The narrow-band characteristic of the emission strongly suggests that the effect is associated with a plasma resonance. From the magnetic field measurements of Ness *et al.* [1980], it is evident that the electron gyrofrequency $f_g \approx 28$ B Hz, where B is in gammas, is only about 100 to 150 Hz in the vicinity of Titan. At frequencies well above the electron gyrofrequency, only two resonances occur in a plasma: the electron plasma oscillation at f_p and the upper hybrid resonance at f_{UHR} . Because $f_{UHR} \approx f_p$ when f_g is small, the emission frequency is very close to the electron plasma frequency. The electron density determination is therefore essentially identical, irrespective of whether the waves are UHR emissions or electron plasma oscillations. The only other possibility that needs to be considered is that the emissions are free-space electromagnetic waves from a remote source. In fact, radio emissions are observed in the 56.2-kHz channel from Saturn (see Figure 2). However, these radio emissions do not have the narrow-band 'spiky' characteristic of the UHR emissions. It seems to us extremely unlikely that the narrow-band bursts identified as UHR emissions could be electromagnetic radiation originating from a remote source. Such an interpretation would involve an extremely unlikely sequence of temporal and frequency variation to reproduce the observed sequence of emissions.

The electron density profile determined from the UHR emissions is shown in greater detail in Figure 4 together with the magnetic field strength obtained from the magnetometer [Ness *et al.*, 1981] and the electron density profile obtained from the plasma instrument [Bridge *et al.*, 1981]. The electric field enhancements, which we identify as UHR emissions, are identified by circles. An electron density scale is shown on the left, using $f = 9\sqrt{n_e}$ kHz. The frequency, time, and corresponding electron density for each of these points are also listed in Table 1. The only criterion used in the identification of these emissions is the presence of a short impulsive emission in a single channel. All emissions of this type are identified, even very weak events that barely exceed the instrument noise level. In constructing the elec-

TABLE 1. UHR Emissions

Time, hr min:s	Frequency, kHz	Electron Density, cm ⁻³
0536:32	5.62	0.39
0537:33	10.0	1.2
0538:30	31.1	12.0
0539:15	56.2	39.0
0540:58	31.1	12.0
0541:59	56.2*	39.0
0542:51	56.2*	39.0
0543:34	31.1	12.0
0543:50	17.8	3.9
0544:42	31.1	12.0
0545:06	17.8	3.9
0545:06	10.0	1.2
0545:13	5.62	0.39

* Radio emission cutoff.

tron density profile a simple, smooth, dashed line was drawn between the UHR points. The only exceptions are the two abrupt cutoffs in the radio emission at 0541:59 and 0542:51 SCET (spacecraft event time). Because these radio emissions originate from Saturn [Daigne *et al.*, this issue], these cutoffs are almost certainly caused by the propagation cutoff of the free-space electromagnetic mode at the electron plasma frequency. The times where these cutoffs occur are assumed to be the times at which the electron plasma frequency (electron density) profile crosses the 56.2-kHz channel. The relatively smooth Saturn radio emissions in the 56.2-kHz channel from 0539:40 to 0541:59 SCET and after 0542:51 SCET indicates that the electron plasma frequency was below 56.2-kHz during these times.

Three pronounced peaks are evident in the electron density profile, the first at about 0539:15 SCET, the second at about 0542:25 SCET, and the third at about 0544:42 SCET. Question marks are shown at the top of the first two peaks. These question marks reflect the fact that the upper limit to the density peaks cannot be determined because no channels are available above 56.2 kHz. For the first peak at 0539:15 SCET, only one strong emission was detected in the 56.2-kHz channel. It is, therefore, highly unlikely that the electron density extended significantly above 39 cm^{-3} at this time. Otherwise, two emissions would be expected, one as the UHR frequency crossed the channel during the rising portion of the density profile and the other during the falling portion of the density profile. For the second peak at 0542:25, two distinct cutoffs were observed in the 56.2-kHz channel, which indicates that the electron density extends well above 39 cm^{-3} . Analysis of the radio astronomy measurements (M. Kaiser, personal communication, 1981) shows that this cutoff did not extend above about 78.0 kHz, which limits the peak electron density to about 75 cm^{-3} . These electron density estimates assume that the radio waves are incident at a large angle to the constant density surface. If the radiation is incident at a shallow angle, as suggested by Daigne *et al.* [this issue], then the electron densities deduced from these propagation cutoffs should be reduced somewhat. We do not, however, believe that a large (more than a factor of 2) reduction is likely because relatively high densities were measured in the same region by the UHR technique (for example, at 0543:34 SCET in the 31.1-kHz channel), with no evidence of a radio emission cutoff in the next higher frequency channel of the type that would be expected if the radio waves were incident at a shallow angle. Probably the electron density is much more complicated and irregular than the simple planar geometry suggested by Daigne *et al.* [this issue]. The third peak at 0544:42 SCET has the lowest electron density, $\sim 12 \text{ cm}^{-3}$, and is the least well defined. The existence of this peak is supported by the fact that a single very weak emission is observed in the 31.1-kHz channel at 0544:42 SCET, which is bracketed by two emissions in the 17.8-kHz channel at 0543:50 and 0545:06 SCET. In interpreting the electron density profile in Figure 4, it should be noted that electron densities can only be determined at the points where a UHR emission or propagation cutoff can be identified. For the time intervals between these points it must be emphasized that the actual electron density profile may deviate significantly from the smooth curve which has been drawn through the points. As discussed earlier, comparisons with the electron density from

the plasma instrument suggest that large density variations may occur in the intervals between the UHR points.

Comparing the electron density profile with the magnetic field strength profile given at the top of Figure 4 shows that the three density peaks occur essentially coincident with three well-defined depressions in the magnetic field. According to the interpretation of Ness *et al.* [1981], the first depression, at about 0539:30 SCET, is the inbound crossing into the magnetic tail of Titan. The approximate direction of the magnetic field is illustrated by the arrows at the top of Figure 4. As can be seen, the magnetic field rotates approximately 90° at this crossing, from a southward direction characteristic of Saturn's field, to a downstream direction characteristic of an induced tail field associated with Titan. The second depression, at 0542:30 SCET, corresponds to the crossing of the neutral sheet which separates the northern (L1) and southern (L2) tail lobes of Titan's magnetotail. The magnetic field rotates 180° at this boundary, from toward to away from Titan. The third depression, at 0544:30 UT, corresponds to the outbound exit from the magnetic tail. The magnetic field again rotates approximately 90° , shifting to a southward direction characteristic of Saturn's field.

3. LOW-FREQUENCY NOISE

In addition to the upper hybrid resonance emissions, several regions of intense low-frequency electric field turbulence were encountered during the Titan flyby. The electric field intensities in the low-frequency spectrum analyzer channels are shown in Figure 5. Three distinct regions of low-frequency noise can be identified: one from 0532:30 to 0538:30, a second from 0539:30 to 0542:15, and a third from 0542:45 to 0545:30 SCET. The first region of intense noise starts about 6 min before closest approach and extends essentially continuously up to the inbound crossing into the magnetic tail M1. A spectrum of this noise, at the point marked A in Figure 5, is shown in Figure 6. As can be seen the spectrum has a broad peak centered at a frequency of about 100 to 200 Hz. The broadband electric field strength is about 0.5 mV m^{-1} . Because this noise is qualitatively similar to the electric field noise found in the magnetosheath at the earth [Rodriguez, 1979] and the ionosheath at Venus [Scarf *et al.*, 1980], we refer to this region as the sheath. However, in contrast to the symmetrical dawn-dusk sheath configuration which exists at the earth and Venus, the sheath at Titan is highly asymmetrical. As can be seen from Figure 5 the strong sheath noise only occurs on the inbound pass. On the outbound pass the noise is essentially undetectable, except for a few isolated bursts indicated by the question marks. These bursts are probably not related to Titan because they occur sporadically throughout the outer magnetosphere of Saturn. On the inbound pass the onset of the sheath noise occurs essentially coincident with an abrupt depression in the magnetic field strength (see the top panel of Figure 5). The abrupt burst of noise that occurs at this time led us to speculate [Gurnett *et al.*, 1981] that this boundary may represent a crossing of a slow-mode shock. However, neither the plasma nor the magnetic field instruments on Voyager confirmed the presence of a shock [Bridge *et al.*, 1981; Ness *et al.*, 1981], so the existence of a shock at this boundary remains doubtful.

Within the tail lobes, another type of low-frequency electric field noise is observed. Typical spectrums of the

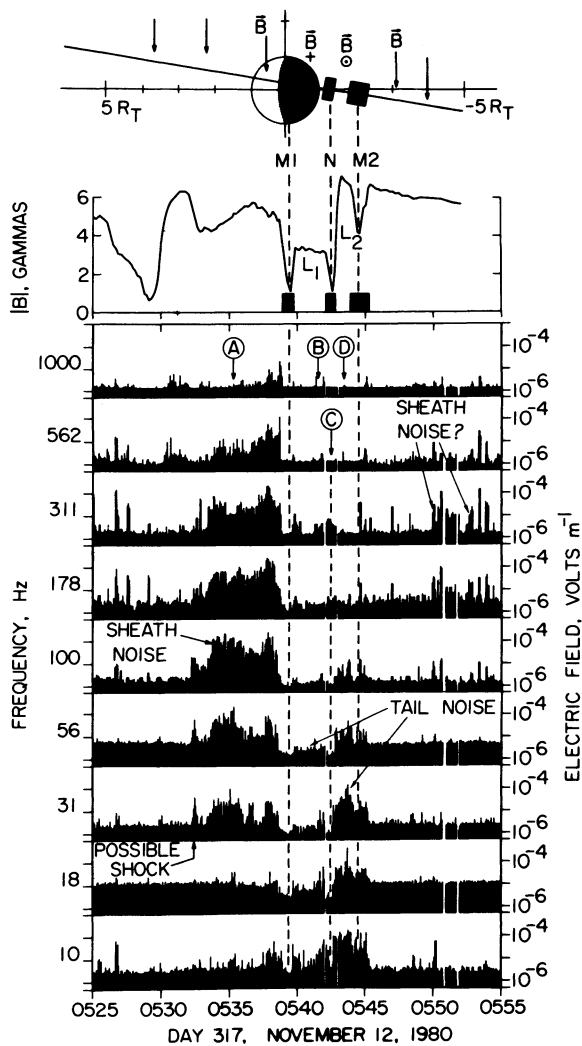


Fig. 5. A comparison of the low-frequency electric field noise and the magnetic field observations in the vicinity of Titan. The sheath noise occurs outside of the tail and is almost completely confined to the inbound leg. Within the northern and southern tail lobes L1 and L2, a much different type of low-frequency noise occurs, confined mainly to frequencies below 100 Hz.

electric field intensities in the tail are shown in Figure 7 at the points marked B, C, and D in Figure 5. Spectrums B and D are in the northern (L1) and southern (L2) lobes, respectively, and spectrum C is in the neutral sheet between the two tail lobes. As can be seen, the noise levels in the neutral sheet are very low, essentially at the instrument noise level. In the tail lobes the electric field intensities are quite large at low frequencies, decreasing more or less monotonically with increasing frequency. The broadband electric field intensity of this noise, integrated over the frequency range from 10 Hz to 1 kHz, is about $100 \mu\text{V m}^{-1}$. The upper frequency limit of the noise is near the electron gyrofrequency, which ranges from 100 to 150 Hz.

4. INTERPRETATION

As discussed in the previous sections the upper hybrid resonance emissions observed in the vicinity of Titan have provided an electron density profile through the wake of Titan. The electron density profile has three distinct peaks: the first corresponding to the entry into the northern tail

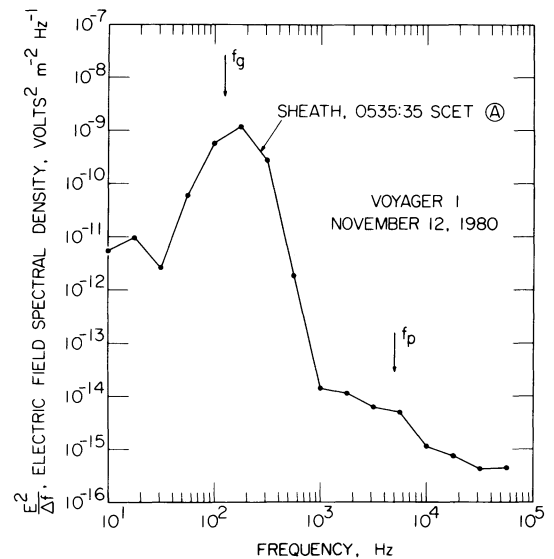


Fig. 6. The electric field spectral density of the sheath noise observed on the inbound leg. The broadband electric field strength of this noise is about 0.5 mV m^{-1} .

lobe, the second corresponding to the crossing of the neutral sheet, and the third corresponding to the exit from the southern tail lobe. Because the electron density at the third peak is smaller than at the first peak, a significant asymmetry appears to be present in the plasma density distribution on the inbound and outbound sides of the magnetic tail. The axis of symmetry of the tail also appears to be skewed about 20° toward Saturn. The maximum electron densities observed in the tail are about 40 cm^{-3} . These electron densities are substantially larger than the peak electron densities of about $\sim 1.5 \text{ cm}^{-3}$ obtained from the MIT plasma instrument, shown at the bottom of Figure 4 [from *Bridge et al.*, 1981]. As pointed out by Bridge et al, the relatively long, 96-s time interval between successive plasma electron measurements

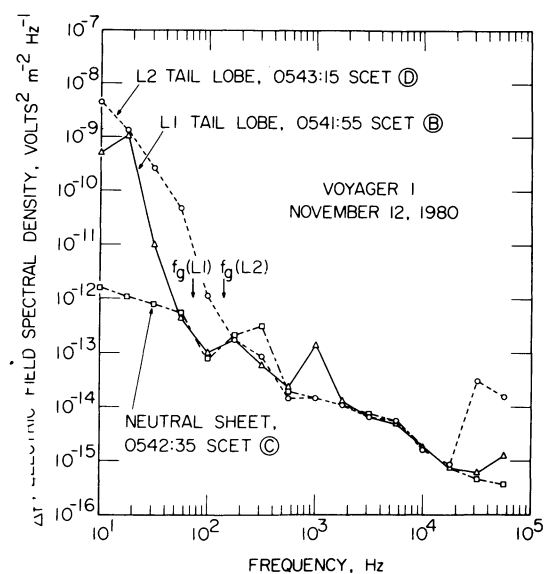


Fig. 7. The electric field spectral density of the low-frequency noise detected in the tail. The noise observed in both the northern (L1) and southern (L2) tail lobes is very similar, rising steeply in intensity toward lower frequencies. In the neutral sheet the intensities are very low, essentially at the instrument noise level.

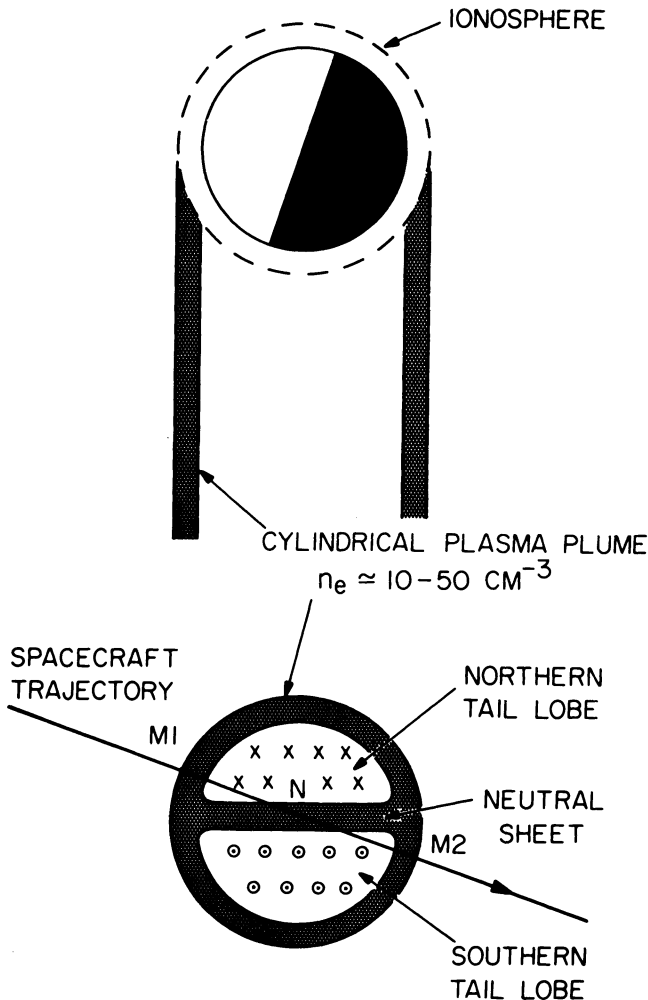


Fig. 8. An interpretation of the electron density profile illustrated in Figure 4. The plasma density peaks at the inbound and outbound tail entries (M1 and M2) are presumed to represent a cylindrical plume of plasma originating from the ionosphere near the limb of Titan. The plasma density peak at the neutral sheet crossing (N) is presumed to represent a sheet of plasma confined between the northern and southern tail lobes, similar to the terrestrial plasma sheet. Because all the measurements are near the equatorial plane, the plasma plume could have either a θ or an H cross section.

makes it impossible for the plasma instrument to resolve small-scale features with durations less than about 96 s. Because the density peaks are very localized, it is therefore possible that the plasma instrument simply missed the three narrow density peaks at 0539:15, 0542:25, and 0544:42 SCET. As can be seen from Figure 4, these highly localized enhancements have a duration of only about 30 s, which is substantially less than the time resolution of the plasma instrument. In other cases it is more difficult to reconcile the two measurements. For example, the UHR point in the northern tail lobe at 0540:58 SCET (see Figure 4) indicates an electron density of about 12 cm^{-3} , whereas a nearby measurement from the plasma instrument indicates an electron density of only 0.5 cm^{-3} . If the UHR measurement is characteristic of the entire tail lobe, then the plasma instrument should indicate a higher density. A possible mutually consistent interpretation is to assume that large density fluctuations were occurring in the tail lobe and that the single point obtained from the upper hybrid emission represents a

single isolated peak. In a future paper we plan to undertake a detailed comparison of the plasma and plasma wave density measurements in order to resolve these interpretational difficulties.

We now consider the possible interpretations of the observed density structure. The observation of localized density enhancements on a spatial scale much smaller than the radius of Titan strongly suggests the existence of narrow plumes of plasma escaping downstream of Titan. The location of the first and third enhancements, on the inbound and outbound sides of the tail, further suggests that this plume may have a cylindrical, sheetlike configuration aligned along the axis of the tail as illustrated in Figure 8. The most likely source of plasma for this plume is the ionosphere of Titan. A somewhat similar cylindrical plume geometry has been reported at Venus by *Brace et al.* [1981] in which clouds of detached ionosphere plasma are swept downstream from the limbs of Venus by the solar wind. Because only a single pass is available at Titan, it is not possible to determine whether the plume is a transient cloudlike feature similar to Venus or a steady state feature. Also, the closure of the plume over the northern and southern polar regions to form a θ -shaped cross section as opposed to an H-shaped cross section is uncertain because of the absence of measurements away from the equatorial plane. The marked asymmetry in the plasma density on the inbound and outbound side of the tail is most simply explained by a day-night asymmetry of Titan's ionosphere. As can be seen in Figure 8, the outbound side of the tail is connected to the nightside of Titan. Since the ionospheric electron density would be expected to be much lower on the nightside of Titan, the lower density of the plasma plume on the outbound side of the tail may be due to the reduced source strength in the nightside ionosphere. On the other hand, if the plasma loss is a transient process with clouds of plasma peeling away from the ionosphere, similar to the situation at Venus, then the apparent asymmetry in the plasma density profile could be due to temporal variations.

The plasma density enhancements observed at the magnetic field depressions associated with Titan's magnetic tail strongly suggest the plasma confinement which occurs in the terrestrial and Jovian plasma sheet. In these cases the plasma pressure in the plasma sheet is balanced by the magnetic field pressure in the adjacent tail lobes. Assuming that this same process is occurring in Titan's magnetic tail, the electron and ion temperatures T_e and T_i of the plasma can be estimated by using the MHD pressure balance equation

$$\frac{1}{2\mu_0} (B_L^2 - B_N^2) = nk(T_e + T_i) \quad (1)$$

where n is the electron density in the neutral sheet and B_L and B_N are the magnetic field strengths in the lobe and neutral sheet, respectively. Using $n = 40 \text{ cm}^{-3}$, $B_L = 5 \gamma$ (average of the northern and southern lobe fields), and $B_N = 1 \gamma$, the sum of the electron and ion temperatures is $T_e + T_i = 1.7 \times 10^4 \text{ K}$. Assuming equal electron and ion temperatures, the plasma temperature is then $T_e = T_i = 8.6 \times 10^3 \text{ K}$. If the electron density is increased to 75 cm^{-3} , the plasma temperature is reduced to $4.1 \times 10^3 \text{ K}$. Further refinements can be made by including the effect of plasma pressure in the tail lobes. However, unless an unusually large temperature difference exists between the lobe and the plasma sheet, the

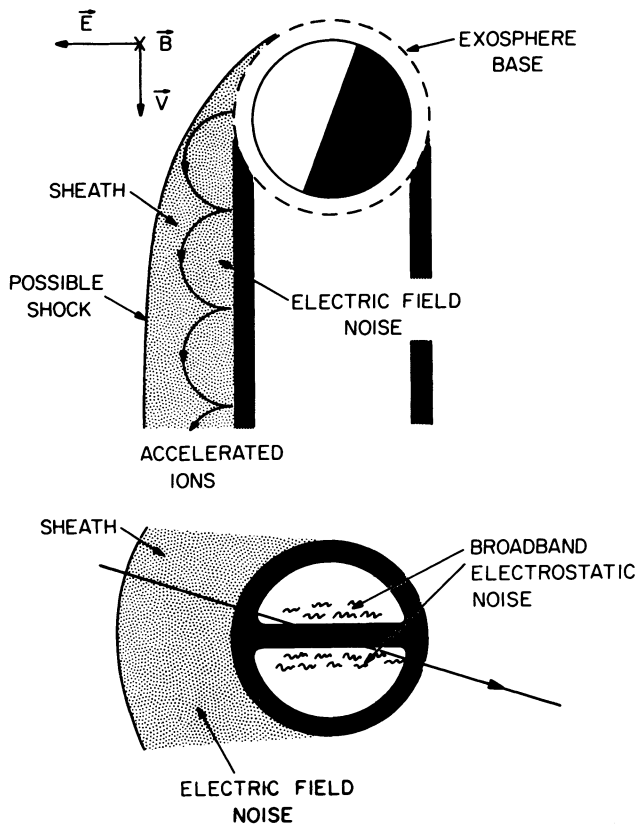


Fig. 9. An interpretation of the sheath noise detected on the inbound leg. This noise is thought to be produced by ions created near the base of the exosphere and accelerated away from Titan by the corotational electric field. This acceleration process would only be operative on the side of Titan facing away from Saturn, which would explain the almost complete absence of this noise on the outbound leg.

plasma sheet temperatures are still less than 10^4 K. These low temperatures are very typical of ionospheric plasma temperatures, thereby providing a strong indication that the plasma is of ionospheric origin. Note that the low temperatures obtained are not consistent with a temperature of several million degrees, which would occur if atmospheric atoms were ionized and accelerated to the nominal magnetospheric flow velocity of 200 km s^{-1} by the corotational electric field. In order for the MHD pressure balance argument used above to be valid, the ion gyroradius must be small in comparison to the thickness of the plasma sheet. For a temperature of 8.6×10^3 K, the gyroradii of H^+ and N^+ ions in a $5\text{-}\gamma$ field is about 17 km and 63 km, respectively. These gyroradii are small in comparison to the estimated plasma sheet thickness of about $0.1 R_T \approx 250 \text{ km}$. Thus the temperatures obtained are consistent with the MHD pressure balance model.

It is useful to try to estimate the velocity of the plasma plume. An upper limit to the plume velocity can be obtained from conservation of momentum. If we assume that all of the momentum of the plasma incident on the face of Titan is converted to momentum of the plume, the plume velocity can be computed from

$$M_m n_m v_m^2 A_T = M_p n_p v_p^2 A_p \quad (2)$$

where M_m , n_m , and v_m are the ion mass, number density, and velocity of the magnetospheric plasma; M_p , n_p , and v_p are

the ion mass, number density, and velocity of the plume; and A_T and A_p are the cross-sectional areas of Titan and the plume, respectively. Using $M_m(\text{H}^+)/M_p(\text{N}^+) = 1/14$, $n_m/n_p = 0.1/40$, $A_T/A_p = 1/0.2$, and $v_m = 200 \text{ km s}^{-1}$, an upper limit to the velocity of the plume is approximately $v_p \approx 6.0 \text{ km s}^{-1}$. This velocity, of course, increases as the cross section for interaction with the magnetospheric plasma increases; however, the time constant for this interaction is expected to be quite long. Furthermore, because Titan probably absorbs a substantial fraction of the incident momentum by viscous interactions with the atmosphere, the velocity of the plume is probably much less than 6.0 km s^{-1} . In the vicinity of Titan the plume velocity is therefore expected to be small in comparison to either the spacecraft velocity, $\sim 17.3 \text{ km s}^{-1}$, or the magnetospheric corotational velocity, $\sim 200 \text{ km s}^{-1}$. The existence of such a relatively cold low-velocity plasma plume may be important in the interpretation of the plasma measurements, since the resulting ion velocity distribution may not be completely within the field of view of the Voyager plasma wave instrument, which does not have a sensor viewing along the spacecraft velocity vector.

From the plume velocity it is possible to estimate the total loss rate of plasma from Titan. Taking the cross section of the plume to be an annular ring with a radius of $1 R_T$ and thickness of $0.1 R_T$, plus a plasma sheet with a cross section of $2 R_T$ by $0.1 R_T$, both with an ion density of 40 cm^{-3} , the total loss rate of ionospheric ions is about 1.2×10^{24} ions s^{-1} . This source strength is somewhat lower than the value given by *Bridge et al.* [1981], mainly because of the lower plume velocity. It can be shown that the estimated loss rate has a negligible effect on the atmosphere of Titan on time scales of the age of the universe. However, as discussed by *Bridge et al.*, this loss may represent a significant input of plasma into the outer magnetosphere of Saturn.

Two apparently different types of plasma wave noise were observed during the Titan flyby, one associated with the sheath region, and the other associated with the tail. Although the sheath noise has many close similarities to the electrostatic noise observed in the magnetosheath of the earth and the ionosheath of Venus, the Titan sheath has a pronounced asymmetry which is not known to be present at the earth and Venus. As can be seen from Figure 5 the sheath noise is very strong on the inbound leg but essentially absent on the outbound leg. This strong asymmetry provides an important clue about the origin of this noise. As discussed by *Bridge et al.*, the inbound side of Titan is the favored region for the acceleration and escape of ions created at the base of the exosphere. The process involved is illustrated in Figure 9. Because the corotational electric field $\mathbf{E} = -\mathbf{V} \times \mathbf{B}$ is directed away from Saturn, any ions created on the side of Titan facing away from Saturn will be accelerated upward out of the atmosphere and carried away by the corotational flow. This ion pickup process would tend to produce a highly unstable hot ion distribution on the side of Titan facing away from Saturn. Evidence for the existence of such an ion distribution has been given by *Bridge et al.* Qualitatively, this region of accelerated ions occurs in the same region where the intense sheath noise is observed. On the other side of Titan the corotational electric field is directed into the atmosphere, thereby strongly inhibiting the escape of ions. This basic asymmetry in the ion escape process provides a simple explanation for the absence of the sheathlike electric

field noise on the outbound leg. Bridge et al. have suggested that the sheath noise may play an important role in thermalizing the accelerated ion distribution.

If the ion escape process is responsible for the sheath noise, several possible instabilities that could cause the noise can be identified. Because the ions accelerated by the corotational electric field tend to produce a nearly monoenergetic ring distribution, the resulting distribution is expected to be highly unstable. In the vicinity of the ionization region, the accelerated ions produce a beam that could generate ion-acoustic waves via a beam-driven ion-acoustic or Buneman mode instability [Stix, 1962]. Downstream of the acceleration region, the positive gradient in the velocity distribution function $\partial f/\partial v_{\perp}$ associated with the ring distribution could provide a free-energy source for the electrostatic ion cyclotron stability. On the basis of the observed frequency spectrum we think that it is most likely that the sheath noise is produced by a current-driven ion-acousticlike instability, since the ion-cyclotron instability occurs at frequencies too low and with Doppler shifts too small to account for the observed frequencies. Because of the large velocity of the corotating plasma, $\sim 200 \text{ km s}^{-1}$, and the short wavelength of ion-acoustic waves, $\lambda > 2\pi \lambda_D \approx 800 \text{ m}$ for $N_e \approx 0.3 \text{ cm}^{-3}$ and $T_e \approx 100 \text{ eV}$ [Hartle et al., this issue], the ion-acoustic turbulence would be Doppler shifted up to frequencies of several hundred Hertz, in agreement with the observed frequency spectrum.

If the sheath noise is not associated with ions accelerated by the corotational electric field, then some other free-energy source is needed, such as currents or nonthermal electron distributions. Magnetic field fluctuations are present in the sheath region [Ness et al., 1981], which could be evidence of currents. However, comparable large-amplitude magnetic field fluctuations exist in the magnetospheric plasma outside of the sheath with no evidence of the noise. Thus it does not appear that the current systems causing these magnetic fluctuations are responsible for the noise. The only evidence of a possible association with nonthermal electron distributions is the fact that the noise occurs near the electron gyrofrequency. It is possible, for example, that the noise could consist of narrow-band emissions at low-order harmonics of the electron gyrofrequency, such as the $(n + 1/2)f_g$ electron cyclotron emissions discussed by Kennel et al. [1970]. However, the broadband impulsive character of the emission evident in Figures 2 and 6 does not support this interpretation. Also, we have no explanation for the marked inbound-outbound asymmetry if the free-energy source for the noise originates in the electron distribution.

The electric field noise observed in the magnetotail of Titan has many characteristics similar to a type of noise called broadband electrostatic noise, which is observed in the terrestrial magnetotail [Gurnett et al., 1976]. As with the Titan noise, the spectrum of the terrestrial broadband electrostatic noise decreases monotonically with increasing frequency, varying approximately as $E^2/\Delta f \sim f^{-2}$, and the largest intensities tend to occur at the outer boundary of the plasma (neutral) sheet. Within the terrestrial neutral sheet the noise levels are also usually very low, as in the neutral sheet of Titan. Unfortunately, although the phenomenology of the terrestrial broadband electrostatic noise is reasonably well known, the physical origin of this noise is poorly understood. At present, only two mechanisms have been

proposed to explain this noise. Ashour-Abdalla and Thorne [1977] have suggested that the noise may be caused by electrostatic ion-cyclotron waves driven by a loss-cone instability, and Huba et al. [1978] have suggested that the noise may be caused by a lower-hybrid drift instability driven by the cross-field current. Because field-aligned currents may exist near the outer boundaries of the plasma sheet it is also possible that the noise may be caused by a current-driven instability such as the electrostatic ion-cyclotron instability [Kindel and Kennel, 1971]. Short wavelengths and large Doppler shifts would then be necessary to explain the observed frequency spectrum.

Acknowledgments. The authors wish to thank N. Ness, J. Scudder, and H. Bridge for several useful discussions concerning the interpretation of the magnetic field and plasma data. The research at the University of Iowa was supported by NASA through contract 954013 with JPL, through grants NGL-16-001-002 and NGL-16-001-043 from NASA headquarters, and by the Office of Naval Research. The research at TRW was supported by NASA through contract 954012 with JPL.

The Editor thanks D. D. Barbosa and R. A. Smith for their assistance in evaluating this paper.

REFERENCES

- Ashour-Abdalla, M., and R. M. Thorne, The importance of electrostatic ion-cyclotron instability for quiet-time proton auroral precipitation, *Geophys. Res. Lett.*, **4**, 45, 1977.
- Acuna, M. H., and N. F. Ness, The magnetic field of Saturn: Pioneer 11 observations, *Science*, **207**, 407, 1980.
- Brace, L. H., R. F. Theis, and W. R. Hoegy, Attached and detached plasmas above the ionopause of Venus and their implications, *Planet. Space Sci.*, in press, 1981.
- Bridge, H. S., et al., Plasma observations near Saturn: Initial results from Voyager 1, *Science*, **212**, 217, 1981.
- Christiansen, P., P. Gough, G. Martelli, J.-J. Block, N. Cornilleau, J. Etcheto, R. Gendrin, D. Jones, C. Beghin, and P. Decreau, GEOS 1: Identification of natural magnetospheric emissions, *Nature*, **272**, 682, 1978.
- Daigne, G., M. Pedersen, M. L. Kaiser, and M. D. Desch, Planetary radio astronomy observations during the Voyager 1 Titan flyby, *J. Geophys. Res.*, this issue.
- Gurnett, D. A., L. A. Frank, and R. P. Lepping, Plasma waves in the distant magnetotail, *J. Geophys. Res.*, **81**, 6059, 1976.
- Gurnett, D. A., W. S. Kurth, and F. L. Scarf, Plasma waves near Saturn: Initial results from Voyager 1, *Science*, **212**, 235, 1981.
- Hartle, R. E., E. C. Sittler, K. W. Ogilvie, J. D. Scudder, A. J. Lazarus, and S. K. Atreya, Titan's ion exosphere observed from Voyager 1, *J. Geophys. Res.*, this issue.
- Hartz, T. R., Low-frequency noise emissions and their significance for energetic particle processes in the polar ionosphere, in *The Polar Ionosphere and Magnetospheric Processes*, p. 151, Gordon and Breach, New York, 1970.
- Huba, J. D., N. T. Gladd, and K. Papadopoulos, Lower-hybrid-drift wave turbulence in the distant magnetotail, *J. Geophys. Res.*, **83**, 5217, 1978.
- Hubbard, R. F., and T. J. Birmingham, Electrostatic emissions between electron gyroharmonics in the outer magnetosphere, *J. Geophys. Res.*, **83**, 4837, 1978.
- Kennel, C. F., F. L. Scarf, R. W. Fredricks, J. H. McGehee, and F. V. Coroniti, VLF electric field observations in the magnetosphere, *J. Geophys. Res.*, **75**, 6136, 1970.
- Kindel, J. M., and C. F. Kennel, Topside current instabilities, *J. Geophys. Res.*, **76**, 3055, 1971.
- Krimigis, S. M., T. P. Armstrong, W. I. Axford, C. O. Bostrom, G. Gloeckler, E. P. Keath, L. J. Lanzerotti, J. F. Carbary, D. C. Hamilton, and E. C. Roelof, Low-energy charged particles in Saturn's magnetosphere: Results from Voyager 1, *Science*, **212**, 225, 1981.
- Kurth, W. S., J. D. Craven, L. A. Frank, and D. A. Gurnett, Intense electrostatic waves near the upper hybrid resonance frequency, *J. Geophys. Res.*, **84**, 4145, 1979.

- Mosier, S. R., M. L. Kaiser, and L. W. Brown, Observations of noise bands associated with the upper hybrid resonance by the IMP 6 radio astronomy experiment, *J. Geophys. Res.*, **78**, 1673, 1973.
- Ness, N. F., M. H. Acuna, R. P. Lepping, J. E. P. Connerney, K. W. Behannon, L. F. Burlaga, and F. M. Neubauer, Magnetic field studies by Voyager 1: Preliminary results at Saturn, *Science*, **212**, 211, 1981.
- Rodriguez, P., Magnetosheath electrostatic turbulence, *J. Geophys. Res.*, **84**, 917, 1979.
- Rönmark, K., H. Borg, P. S. Christiansen, M. P. Gough, and D. Jones, Banded electron cyclotron harmonic instability—A first comparison of theory and experiment, *Space Sci. Rev.*, **22**, 401, 1978.
- Scarf, F. L., and D. A. Gurnett, A plasma wave investigation for the Voyager mission, *Space Sci. Rev.*, **21**, 289, 1977.
- Scarf, F. L., W. W. L. Taylor, C. T. Russell, and R. C. Elphic, Pioneer Venus plasma wave observations: The solar wind-Venus interaction, *J. Geophys. Res.*, **85**, 7599, 1980.
- Shaw, R. R., and D. A. Gurnett, Electrostatic noise bands associated with the electron gyrofrequency and plasma frequency in the outer magnetosphere, *J. Geophys. Res.*, **80**, 4259, 1975.
- Smith, E. J., L. Davis, Jr., D. E. Jones, P. J. Coleman, Jr., D. S. Colburn, P. Dyal, and C. P. Sonett, Saturn's magnetic field and magnetosphere, *Science*, **207**, 407, 1980.
- Stix, T., *The Theory of Plasma Waves*, McGraw-Hill, New York, 1962.
- Tyler, G. L., V. R. Eshleman, J. D. Anderson, G. S. Levy, G. F. Lindal, G. E. Wood, T. A. Croft, Radio science investigations of the Saturn system with Voyager 1: Preliminary results, *Science*, **212**, 201, 1981.
- Vogt, R. E., D. L. Chenette, A. C. Cummings, T. L. Garrard, E. C. Stone, A. W. Schardt, J. H. Trainor, N. Lal, and F. B. McDonald, Energetic charged particles in Saturn's magnetosphere: Voyager 1 results, *Science*, **212**, 231, 1981.
- Walsh, D., F. T. Haddock, and H. F. Schulte, Cosmic radio intensities at 1.225 and 2.0 Mc measured up to an altitude of 1700 km, *Space Res.*, **4**, 935, 1964.

(Received June 18, 1981;
revised October 8, 1981;
accepted October 12, 1981.)